

Radiative forcing by forest and subsequent feedbacks in the early Eocene climate

U. Port et al.

Radiative forcing by forest and subsequent feedbacks in the early Eocene climate

U. Port¹, M. Claussen^{1,2}, and V. Brovkin¹

¹Max Planck Institute for Meteorology, Hamburg 20146, Germany

²Meteorological Institute, University of Hamburg, Hamburg 20146, Germany

Received: 2 March 2015 – Accepted: 13 March 2015 – Published: 30 March 2015

Correspondence to: U. Port (ulrike.port@mpimet.mpg.de)

Published by Copernicus Publications on behalf of the European Geosciences Union.

Title Page

Abstract

Introduction

Conclusions

References

Tables

Figures

◀

▶

◀

▶

Back

Close

Full Screen / Esc

Printer-friendly Version

Interactive Discussion

Abstract

Using the Max Planck Institute for Meteorology Earth System Model, we investigate the forcing of forests and the feedback triggered by forests in the pre-industrial climate and in the early Eocene climate (about 54 to 52 million years ago). Other than the interglacial, pre-industrial climate, the early Eocene climate was characterised by high temperatures which led to almost ice-free poles. We compare simulations in which all continents are covered either by dense forest or by bare soil. To isolate the effect of soil albedo, we choose either bright soils or dark soils, respectively. Considering bright soil, forests warm in both, the early Eocene climate and the current climate, but the warming differs due to differences in climate feedbacks. The lapse-rate and water-vapour feedback is stronger in early Eocene climate than in current climate, but strong and negative cloud feedbacks and cloud masking in the early Eocene climate outweigh the stronger positive lapse-rate and water-vapour feedback. In the sum, global mean warming is weaker in the early Eocene climate. Sea-ice related feedbacks are weak in the almost ice-free climate of the early Eocene leading to a weak polar amplification. Considering dark soil, our results change. Forests cools stronger in the early Eocene climate than in the current climate because the lapse-rate and water-vapour feedback is stronger in the early Eocene climate while cloud feedbacks and cloud masking are equally strong in both climates. The different temperature change by forest in both climates highlights the state-dependency of vegetation's impact on climate.

1 Introduction

During the early Eocene (about 54 to 52 million years ago), climate was much warmer than today. Tropical temperatures were 5 to 6 K higher (Pearson et al., 2007), and polar temperatures were above the freezing point during most time of the year leading to almost ice-free poles (Hutchison, 1982; Markwick, 1994; Ivany et al., 2006; Zachos et al., 1992). The major forcing for the warm climate was a higher atmospheric CO₂

CPD

11, 997–1029, 2015

Radiative forcing by forest and subsequent feedbacks in the early Eocene climate

U. Port et al.

Title Page

Abstract

Introduction

Conclusions

References

Tables

Figures

◀

▶

◀

▶

Back

Close

Full Screen / Esc

Printer-friendly Version

Interactive Discussion



Radiative forcing by forest and subsequent feedbacks in the early Eocene climate

U. Port et al.

Title Page	
Abstract	Introduction
Conclusions	References
Tables	Figures
◀	▶
◀	▶
Back	Close
Full Screen / Esc	
Printer-friendly Version	
Interactive Discussion	

concentration than today (Heinemann et al., 2009), but also other factors may have contributed to the warm climate such as altered orbital parameters (Lawrence et al., 2003; Sewall and Sloan, 2004), an increased ocean heat transport (Barron, 1987), and different bathymetry and topography (Sewall et al., 2000). We investigate the impact of vegetation on the early Eocene climate.

Flora fossils indicate that forests dominated the vegetation cover during the early Eocene (Wolfe, 1985). Forest affects climate by taking up CO₂ and by changing the land–atmosphere fluxes (heat, moisture, momentum, and energy). The latter is called the biogeophysical effect of forest. For present-day climate, the biogeophysical effect of forest is well understood. In the high latitudes, forest tends to increase temperature by masking the bright snow cover and, thereby, reducing surface albedo (Bonan, 1992, 2008; Betts and Ball, 1997). The warming is amplified by the sea ice-albedo feedback (Brovkin et al., 1999, 2009; Claussen et al., 2001; Fraedrich et al., 2005). In the tropics, forest tends to reduce temperature by enhancing latent heat flux and increasing cloud cover (Claussen et al., 2001; Bala et al., 2007; Bathiany et al., 2010). Considering the warm early Eocene climate, we assume that the biogeophysical effect changes. We test this hypothesis using the Max Planck Institute for Meteorology Earth System Model (MPI-ESM).

We simulate both, the early Eocene climate and the pre-industrial climate, with dense forest on all continents and with bare soil on all continents, respectively. Based on the differences in temperature and radiative flux between the respective “forest world” and the respective “desert world”, we derive the radiative forcing by forests and the subsequent climate feedbacks. We expect that the radiative forcing by forest depends on the soil albedo. To isolate the impact of soil albedo on the radiative forcing by forest, we simulate the desert world two times. In a first case, we assume a homogeneous soil albedo of 0.1, which is approximately the albedo of volcanic rocks and granite bedrock (Warner, 2004). In this case, soil and forest have similarly low values of albedo. In a second case, we assume a homogeneous soil albedo of 0.4. The bright soil has a much higher albedo than the forest.



For the early Eocene climate and the pre-industrial climate, we prescribe an atmospheric CO₂ concentration of 560 and 280 ppm, respectively. The respective CO₂ concentration is assumed in the forest world and in the desert worlds. In other words, we neglect the CO₂ uptake by forest and focus on the biogeophysical effect of forest.

2 Model and experiments

The MPI-ESM consists of the atmospheric general circulation model ECHAM6 (Stevens et al., 2013), the Max Planck Institute Ocean Model (MPIOM) (Jungclaus et al., 2013), the land surface scheme JSBACH (Reick et al., 2013), and the ocean biogeochemistry model HAMOCC (Ilyina et al., 2013). ECHAM6 and JSBACH run in a horizontal resolution of T31, which corresponds to approximately 3.75° × 3.75°. ECHAM6 considers 31 levels in the vertical up to 10 hPa. The ocean grid has a resolution of about 3° and consists of 40 levels in depth.

To simulate the early Eocene climate, we use the maps of orography and bathymetry by Bice and Marotzke (2001) which Heinemann et al. (2009) interpolated from the original resolution of 2° × 2° to the model resolution of T31. The orography map lacks information on sub-grid orography. Hence, ECHAM6 cannot parametrise sub-grid interactions of atmospheric flow with orography (Stevens et al., 2013) and so we switch off the module for sub-grid orographic drag and wave generation. The distribution of continents requires to shift the regular MPIOM north pole of the ocean grid to Palaeo-Asia and the grid south pole to Palaeo-South America.

Following Heinemann et al. (2009), the atmospheric CO₂ concentration is fixed to 560 ppm (Table 1), which represents the lower limit of reconstructions (Zachos et al., 2001; Beerling and Royer, 2011). Estimates of other greenhouse gases are absent for the early Eocene. Thus, we proceed as Heinemann et al. (2009) and prescribe pre-industrial values for methane and nitrous oxide in the early Eocene atmosphere (Table 1). Orbital parameters fluctuate on a shorter time scale than the early Eocene period (Laskar et al., 2004). Hence, a specific set of orbital parameters for this period

Radiative forcing by forest and subsequent feedbacks in the early Eocene climate

U. Port et al.

Title Page

Abstract

Introduction

Conclusions

References

Tables

Figures



Back

Close

Full Screen / Esc

Printer-friendly Version

Interactive Discussion



is lacking. We decide to use a pre-industrial orbit in our early Eocene simulations. This approach limits the differences between the early Eocene and the pre-industrial boundary conditions to the distribution of continents, the bathymetry, the appearance of ice sheets, and the atmospheric CO₂ concentration.

We perform the same three simulations with the described early Eocene boundary conditions and with pre-industrial boundary conditions (Table 2). In the *dark desert world* and in the *bright desert world*, no vegetation occurs on all continents during the simulated 400 years. Both simulations differ concerning the assumed soil albedo. While all soils have an albedo of 0.1 in the dark desert world, all soils have an albedo of 0.4 in the bright desert world.

In the *forest world*, all ice-free continents are completely covered with forests. The vegetation cover is static and the leaf area index (LAI) is constant throughout the whole simulation independently of season, temperature, and water availability. We distinguish between tropical and extra-tropical trees (Fig. 1). Tropical trees have a LAI of 7 and a roughness length of 2 m. Extra-tropical trees have a LAI of 5 and a roughness length of 1 m. The soil albedo does not matter in the forest world which was tested by simulating the forest world climate with low and high soil albedo, respectively. Both soil albedo values reveal the same climate (not shown) because trees completely mask the soil leading to a land surface albedo of approximately 0.12 in snow-free regions in the forest world.

3 Methods

We aim to compare the impact of forest on the early Eocene climate and on the pre-industrial climate. For this purpose, we compare the forest world simulation to the desert world simulations in both climates. All simulations run for 400 years and climate is not in equilibrium at the end of the simulations. To estimate the impact of forest on climate from these transient simulations anyway, we quantify the radiative forcing by

Radiative forcing by forest and subsequent feedbacks in the early Eocene climate

U. Port et al.

Title Page

Abstract

Introduction

Conclusions

References

Tables

Figures



Back

Close

Full Screen / Esc

Printer-friendly Version

Interactive Discussion



forest and the subsequent climate feedbacks using the linear regression approach by Gregory et al. (2004). This Section introduces the linear regression approach.

3.1 Radiative forcing and climate feedbacks

At the beginning of each simulation, we change the vegetation cover and the soil albedo drastically. The modification of the land surface acts as an external forcing on the climate system and perturbs the radiation balance at the top of the atmosphere (TAO). During the simulation, the perturbation in the TOA radiation balance, ΔR , changes surface temperature. Temperature changes feed back to ΔR due to internal mechanisms in the climate system. In the global mean, ΔR relates approximately linearly to the changes in surface temperature, ΔT ,

$$\Delta R(t) = \Delta Q + \lambda \Delta T(t). \quad (1)$$

The instantaneous response of the radiation balance to the modification of the land surface is the radiative forcing, ΔQ . The climate feedback parameter, λ , quantifies the strength of feedbacks between temperature and ΔR .

The model simulations provide pairs of ΔR^i and ΔT^i for each year, i . Figure 2 shows the points of $(\Delta T^i, \Delta R^i)$ for the early Eocene dark desert world simulation. The initial climate is an equilibrium climate simulated with savanna on all continents. In the first year of the shown simulation, savanna is replaced by dark bare soil, and the simulated climate progressively approaches a new equilibrium. The straight line fitted to the points of $(\Delta T^i, \Delta R^i)$ reveals the parameters in Eq. (1) (Gregory et al., 2004). At the intersection of the regression line with the ΔR axis, ΔR is the radiative forcing ΔQ . The slope of the regression line is the feedback parameter λ . λ is negative here indicating that feedbacks counteract the perturbation in the TOA radiation balance. In other words, feedbacks stabilise climate. The new equilibrium is estimated from the intersection of ΔR with the ΔT axis, i.e. the perturbation ΔR approaches zero, and the new

Radiative forcing by forest and subsequent feedbacks in the early Eocene climate

U. Port et al.

Title Page

Abstract

Introduction

Conclusions

References

Tables

Figures

◀

▶

◀

▶

Back

Close

Full Screen / Esc

Printer-friendly Version

Interactive Discussion



equilibrium temperature is

$$\Delta T^{\text{eq}} = -\frac{\Delta Q}{\lambda}. \quad (2)$$

The linear regression approach is only valid when feedbacks are constant in time. The slope of the regression line, however, decreases with time (Gregory et al., 2004).

5 For the first decades after a perturbation, however, Gregory et al. (2004) find a constant slope. As is now customary, we consider the first 150 years of our simulation for the regression (Andrews et al., 2012).

For the forest world simulation, the linear regression approach reveals the radiative forcing and the feedbacks by afforesting savanna-like vegetation. However, we aim to
10 estimate the radiative forcing and the feedbacks from afforesting deserts on all continents. Hence, we modify the linear regression approach in the way that we combine the forest world simulation with the desert world simulations. Let ΔR_d be the perturbation of the net ToA radiation in the case of replacing savanna with desert, and let ΔR_f be the perturbation in the case of replacing savanna with forest. In the linear approach,
15 the difference, ΔR_{fd} , is the perturbation due to replacing deserts by a complete forest cover. For each year in our simulation, i , we receive

$$\Delta R_{fd}^i = \Delta R_f^i - \Delta R_d^i, \quad (3)$$

Consistently, we subtract the temperature differences of the two perturbation experiment to obtain

$$\Delta T_{fd}^i = \Delta T_f^i - \Delta T_d^i = T_f^i - T_d^i. \quad (4)$$

20 Considering Eq. (1), the regression line to the points $(\Delta T_{fd}, \Delta R_{fd})$ is

$$\Delta R_{fd} = \Delta Q_{fd} + \lambda_{fd} \Delta T_{fd}. \quad (5)$$

The radiative forcing of afforesting the desert world is expressed by ΔQ_{fd} . The according feedback parameter is λ_{fd} . The equilibrium temperature response, $\Delta T_{fd}^{\text{eq}}$, is
25 approximated by $\Delta R_{fd}(\Delta T_{fd} = 0)$.

CPD

11, 997–1029, 2015

Radiative forcing by forest and subsequent feedbacks in the early Eocene climate

U. Port et al.

Title Page

Abstract

Introduction

Conclusions

References

Tables

Figures

◀

▶

◀

▶

Back

Close

Full Screen / Esc

Printer-friendly Version

Interactive Discussion



Radiative forcing by forest and subsequent feedbacks in the early Eocene climate

U. Port et al.

Title Page

Abstract

Introduction

Conclusions

References

Tables

Figures

◀

▶

◀

▶

Back

Close

Full Screen / Esc

Printer-friendly Version

Interactive Discussion

The term on the right hand side consists of the Stefan–Boltzmann constant, σ , the global mean surface temperature in Kelvin [K], T , and the emissivity of the atmosphere, ϵ . The emissivity describes the strength of the greenhouse effect and varies depending on the climate state. We estimate ϵ from the ratio of long-wave radiation escaping at the top of the atmosphere to long-wave radiation emitted by the surface. At the beginning of the simulations, ϵ is 0.585 and 0.541 in the pre-industrial climate and in the early Eocene climate which reflects the stronger greenhouse effect in the warmer early Eocene climate. The corresponding global mean surface temperatures are 287 and 297 K. Considering these values, Eq. (11) reveals a λ_p of -3.1 and $-3.3 \text{ W m}^{-2} \text{ K}^{-1}$ in the pre-industrial climate and in the early Eocene climate, respectively. Assuming that feedbacks act linearly, we subtract λ_p from λ_{LWcl} . The remaining feedback parameter is mainly the lapse-rate and water-vapour feedback which we name $\lambda_{\text{WV+LR}}$.

We quantify the uncertainty of forcings and feedbacks in terms of the 95 % confidence interval which we assess using bootstrapping. We randomly select 150 pairs of differences in temperature and TOA radiative flux out of the first 150 years of our simulation. Each pair of our simulation can be selected several times. We repeat the resampling 10 000 times. From each time, we estimate the feedbacks and forcings and sort the resulting 10 000 values. Truncating the upper and lower 2.5 % provides the 95 % confidence interval.

4 Results

Based on the regression approach, we estimate radiative forcing of forestation and climate feedbacks. First, we compare the forest world to the bright desert world and discuss differences in radiative forcing and climate feedbacks between the early Eocene climate and the pre-industrial climate. Second, we compare the forest world to the dark desert world. In this case, forest and soil have about the same albedo which cancels the albedo effect of forest in snow-free regions. We relate the differences in radiative

Radiative forcing by forest and subsequent feedbacks in the early Eocene climate

U. Port et al.

[Title Page](#)

[Abstract](#)

[Introduction](#)

[Conclusions](#)

[References](#)

[Tables](#)

[Figures](#)

[◀](#)

[▶](#)

[◀](#)

[▶](#)

[Back](#)

[Close](#)

[Full Screen / Esc](#)

[Printer-friendly Version](#)

[Interactive Discussion](#)

cover compensates the surface albedo reduction. Figure 5 illustrates the compensation of surface albedo reduction. Shown are the difference in planetary albedo and in cloud cover between the first year of the forest world simulation and the first year of the desert world simulation. In general, planetary albedo over land decreases due to forests, but in the tropics, cloud cover increases leading to a weak decrease in planetary albedo.

The cloud masking effect is an artefact which results from separating full-sky radiation into the clear-sky component and the cloud component. In case a dense cloud cover occurs in the forest world and in the desert world, full-sky short-wave radiative forcing will be weak. Clear-sky radiation, however, will be strongly positive due to the lower surface albedo in the forest world than in the desert world. Deriving the cloud forcing from the weak full-sky radiative forcing and the strongly positive clear-sky radiation reveals a strongly negative cloud radiative forcing even though cloud cover did not change. Our approach do not allow to disentangle cloud adjustment and cloud masking. Nevertheless, we assume that a considerable part of the ΔQ_{SWcl} results from the cloud masking effect.

Feedbacks stabilise the early Eocene climate stronger than the pre-industrial climate as the steeper slope of the regression line in Fig. 3 illustrates. Stronger stabilising feedbacks lead to a smaller equilibrium temperature response in the early Eocene climate and to a smaller temperature difference between the bright desert world and the forest world at the end of the simulations (Table 3). This result is surprising because Caballero and Huber (2013) finds that the same forcing causes a similarly strong net feedback for the warm early Palaeogene climate (about 65 to 35 million years ago) as for present-day climate.

We analyse the single components of the net feedback to identify the reason for the different strength in net feedback in both climate states. The short-wave clear-sky feedback parameter, λ_{SWCS} , is significantly smaller in the early Eocene climate than in the pre-industrial climate (Fig. 6). This feedback mainly refers to changes in the sea-ice cover and snow cover together with the short-wave contribution of the water-vapour feedback. We expect that the ice-albedo feedback is weak in the early Eocene

Radiative forcing by forest and subsequent feedbacks in the early Eocene climate

U. Port et al.

Title Page

Abstract

Introduction

Conclusions

References

Tables

Figures

◀

▶

◀

▶

Back

Close

Full Screen / Esc

Printer-friendly Version

Interactive Discussion

climate because permanent sea-ice is absent and snow occurs only seasonally. The small λ_{SWCS} agrees with this expectations. Also zonal mean temperature differences between the forest world and the desert world indicate a weak ice-albedo feedback as forests warm the northern high latitudes much less in the early Eocene climate than in the pre-industrial climate (Fig. 7).

$\lambda_{\text{WV+LR}}$ largely quantifies the sum of the negative lapse-rate feedback and the positive water-vapour feedback. This feedback parameter is larger in the early Eocene climate than in the pre-industrial climate indicating either a weaker lapse-rate feedback, a stronger water-vapour feedback, or both. This result agrees with Meraner et al. (2013) who suggest that the water-vapour feedback becomes stronger with warming.

Largest differences in the feedback parameters appear in the short-wave cloud feedback parameter, λ_{SWcl} , which is $-0.8 \text{ W m}^{-2} \text{ K}^{-1}$ in the early Eocene climate and $0.1 \text{ W m}^{-2} \text{ K}^{-1}$ in the pre-industrial climate. Even considering the large uncertainty in the estimate, λ_{SWcl} differs significantly in both climates. The differences in λ_{SWcl} indicate that the cloud albedo feedback is stronger and of opposite sign in the early Eocene climate than in the pre-industrial climate. λ_{SWcl} , however, also includes masking effects of clouds which weakens the result on the climate-dependent cloud albedo feedback.

To identify the reason for the different λ_{SWcl} in both climates, we separate the difference in the short-wave cloud radiative flux between the forest world and the bright desert world, ΔR_{SWcl} , into ΔR_{SWcl} above the oceans and above the continents (similar to Andrews et al., 2012). Over land, the λ_{SWcl} is nearly of the same strength in both climate states as the slope of the regression lines in Fig. 8a illustrates. Over the oceans, λ_{SWcl} is positive in the pre-industrial climate and negative in the early Eocene climate (Fig. 8b). The different sign in λ_{SWcl} indicates a different structure in cloud cover changes with changes in sea-surface temperature in both climates.

The regression line in Fig. 8b considers the first 150 years of the simulations but do not represent the last 250 years. Consistently with previous studies (Senior and Mitchell, 2000), this behaviour indicates a time-dependent cloud feedback which is not captured by the linear regression approach.

4.2 Forestation of a dark desert world

We showed above that forest changes temperature by lowering surface albedo and enhancing cloud cover. To isolate these two effects, we now set the soil albedo in the desert world to 0.1 which is about the albedo of forest. In other words, the albedo effect of forest is weak in snow-free regions. Relative to the dark desert world, forests reduce temperature by 4.2 and 3.0 K until the end of the early Eocene simulations and until the end of the pre-industrial simulations, respectively (Table 4). The cooling results from a negative radiative forcing of about 3 W m^{-2} in both climate states (Fig. 9).

The main contributor to the net radiative forcing is ΔQ_{SWcl} (Fig. 10) which composes of the cloud adjustment and the cloud masking effect. Above, we argue that cloud adjustment by forest is strong when the soil albedo is high in the desert world. In this case, forest reduces surface albedo and an increased cloud cover compensates the reduction in surface albedo (Sect. 4.1). Now, we consider a low soil albedo which is close to the albedo of forest. Hence, surface albedo changes by forest are weak leading to a weak compensation effect by an increased cloud cover. Presumably, the weak compensation effect leads to a weaker cloud adjustment than in the bright-soil case which might explain the smaller ΔQ_{SWcl} .

In contrast to the bright-soil case, net feedback is equally strong in the early Eocene climate as in the pre-industrial climate (Table 4). The separation into the single components reveals that $\lambda_{\text{LR+VW}}$ is larger in the early Eocene climate than in the pre-industrial climate, while λ_{SWcs} is smaller. Even though the differences in $\lambda_{\text{LR+VW}}$ and λ_{SWcs} compensate on the global scale, they are relevant on the regional scale. The larger $\lambda_{\text{LR+VW}}$ in the early Eocene climate indicates a stronger lapse-rate and water-vapour feedback which amplifies the cooling by forests on a global scale. The smaller λ_{SWcs} likely indicates a weaker sea-ice albedo feedback which leads to a weaker polar amplification of the cooling by forest than in the pre-industrial climate.

CPD

11, 997–1029, 2015

Radiative forcing by forest and subsequent feedbacks in the early Eocene climate

U. Port et al.

Title Page

Abstract

Introduction

Conclusions

References

Tables

Figures

◀

▶

◀

▶

Back

Close

Full Screen / Esc

Printer-friendly Version

Interactive Discussion

5 Conclusions

Our results underline that the radiative forcing by changes in vegetation cover and the feedbacks in the climate system depend on the climate state. In the current interglacial climate, forest exerts a positive radiative forcing when soil has a much higher albedo than forest. The major effect is the surface albedo reduction by forest, which is partly offset by a negative cloud adjustment and masking effect. The positive net radiative forcing results in a warming and induces climate feedbacks: The lapse-rate and water-vapour feedback enhances warming on global scale; and the sea-ice albedo feedback amplifies warming in the northern high latitudes.

In the nearly ice-free, warm climate of the early Eocene, forests exert a similar radiative forcing, but climate feedbacks differ considerably. The sea-ice albedo feedback is weaker in the early Eocene climate than in current climate leading to a weaker warming in the northern high latitudes. The positive lapse-rate and water-vapour feedback is stronger than in current climate. Negative cloud-related feedbacks, however, are also stronger and outweigh the stronger positive lapse-rate and water-vapour feedback. In the sum, climate feedbacks stabilise the early Eocene climate stronger than the current climate.

Assuming that soils have an albedo close to the albedo of forest, the major radiative forcing is the cloud adjustment and masking effect which is equally strong in the early Eocene climate as in the pre-industrial climate. The resulting cooling, however, differs in both climates because feedbacks are differently strong. Like in the bright soil case, the positive lapse-rate and water-vapour feedback is stronger in the early Eocene climate, but this time cloud feedbacks and masking effects are of similar strength in both climates. Hence, the net feedback stabilise the early Eocene climate less leading to a stronger cooling than in the current climate. Polar amplification is still weak in the early Eocene climate due to weak sea-ice related feedbacks.

In our study, plant functional types are considered to be the same for early Eocene climate and for pre-industrial climate. We assume that this simplification will affect the

Radiative forcing by forest and subsequent feedbacks in the early Eocene climate

U. Port et al.

Title Page

Abstract

Introduction

Conclusions

References

Tables

Figures

◀

▶

◀

▶

Back

Close

Full Screen / Esc

Printer-friendly Version

Interactive Discussion



Radiative forcing by forest and subsequent feedbacks in the early Eocene climate

U. Port et al.

Title Page

Abstract

Introduction

Conclusions

References

Tables

Figures

◀

▶

◀

▶

Back

Close

Full Screen / Esc

Printer-friendly Version

Interactive Discussion

results of our study, at least in the qualitative sense, only little. We prescribe extreme land cover differences between completely forested and completely deserted continents. This difference is likely to cause much stronger effects than the difference in the physiology between current forests and early Eocene forests.

As climate has ever been changing through Earth's history, it is to be assumed that the impact of vegetation on climate is likely to change. Hence, attempts to infer potential changes in the future from processes that occurred in the past are challenging. Studies of past climates, however, help to understand the dynamics of the climate system which is a prerequisite for application of models to explore potential future changes.

Acknowledgements. We are grateful for comments and help by Bjoern Stevens and Thorsten Mauritsen. Further, we thank Veronika Gayler and Helmuth Haak for technical support. The anonymous reviewer improved the clarity of this paper. This work used computational resources by Deutsches Klima Rechenzentrum (DKRZ) and was supported by the Max Planck Gesellschaft (MPG).

The article processing charges for this open-access publication have been covered by the Max Planck Society.

References

- Andrews, T., Gregory, J., Webb, M., and Taylor, K.: Forcing, feedbacks and climate sensitivity in CMIP5 coupled atmosphere-ocean climate models, *Geophys. Res. Lett.*, 39, doi:10.1029/2012GL051607, available at: <http://tinyurl.sfx.mpg.de/t8j2>, 2012. 1003, 1004, 1008
- Bala, G., Caldeira, K., Wickett, M., Phillips, T. J., and Lobell, D. B.: Combined climate and carbon-cycle effects of large-scale deforestation, *P. Natl. Acad. Sci. USA*, 104, 6550–6555, 2007. 999
- Barron, E. J.: Eocene equator-to-pole surface ocean temperatures: a significant climate problem?, *Paleoceanography*, 2, 729–739, 1987. 999

Radiative forcing by forest and subsequent feedbacks in the early Eocene climate

U. Port et al.

[Title Page](#)
[Abstract](#)
[Introduction](#)
[Conclusions](#)
[References](#)
[Tables](#)
[Figures](#)




[Back](#)
[Close](#)
[Full Screen / Esc](#)
[Printer-friendly Version](#)
[Interactive Discussion](#)


- Bathiany, S., Claussen, M., Brovkin, V., Raddatz, T., and Gayler, V.: Combined biogeophysical and biogeochemical effects of large-scale forest cover changes in the MPI earth system model, *Biogeosciences*, 7, 1383–1399, doi:10.5194/bg-7-1383-2010, 2010. 999
- Beerling, D. and Royer, D.: Convergent Cenozoic CO₂ history, *Nat. Geosci.*, 4, 418–420, doi:10.1038/ngeo1186, available at: <http://tinyurl.sfx.mpg.de/t5fm>, 2011. 1000
- Betts, A. K. and Ball, J. H.: Albedo over the boreal forest, *J. Geophys. Res.-Atmos.*, 102, 28901–28909, doi:10.1029/96JD03876, 1997. 999
- Bice, K. L. and Marotzke, J.: Numerical evidence against reversed thermohaline circulation in the warm Paleocene/Eocene ocean, *J. Geophys. Res.*, 106, 11529–11542, 2001. 1000, 1015
- Bonan, G. B.: Effects of boreal forest vegetation on global climate, *Nature*, 359, 716–718, 1992. 999
- Bonan, G. B.: Forests and climate change: forcings, feedbacks, and the climate benefits of forests, *Science*, 320, 1444–1449, 2008. 999
- Brovkin, Ganopolski, A., Claussen, M., Kubatzki, C., and Petoukhov, V.: Modelling climate response to historical land cover change, *Global Ecol. Biogeogr.*, 8, 509–517, doi:10.1046/j.1365-2699.1999.00169.x, available at: <http://tinyurl.sfx.mpg.de/tyey>, 1999. 999
- Brovkin, V., Raddatz, T., and Reick, C. H.: Global biogeophysical interactions between forest and climate, *Geophys. Res. Lett.*, 36, L07405, doi:10.1029/2009GL037543, 2009. 999
- Caballero, R. and Huber, M.: State-dependent climate sensitivity in past warm climates and its implications for future climate projections, *P. Natl. Acad. Sci. USA*, 110, 14162–14167, doi:10.1073/pnas.1303365110, available at: <http://tinyurl.sfx.mpg.de/u3k4>, 2013. 1007
- Claussen, M., Brovkin, V., and Ganopolski, A.: Biogeophysical versus biogeochemical feedbacks of large-scale land cover change, *Geophys. Res. Lett.*, 28, 1011–1014, 2001. 999
- Fraedrich, K., Jansen, H., Kirk, E., and Lunkeit, F.: The Planet Simulator: green planet and desert world, *Meteorol. Z.*, 14, 305–314, doi:10.1127/0941-2948/2005/0044, available at: <http://tinyurl.sfx.mpg.de/tczv>, 2005. 999
- Gregory, J., Ingram, W., Palmer, M., Jones, G., and Stott, P.: A new method for diagnosing radiative forcing and climate sensitivity, *Geophys. Res. Lett.*, 31, L03205, doi:10.1029/2003GL018747, available at: <http://tinyurl.sfx.mpg.de/tcyk>, 2004. 1002, 1003
- Heinemann, M., Jungclaus, J. H., and Marotzke, J.: Warm Paleocene/Eocene climate as simulated in ECHAM5/MPI-OM, *Clim. Past*, 5, 785–802, doi:10.5194/cp-5-785-2009, 2009. 999, 1000

Radiative forcing by forest and subsequent feedbacks in the early Eocene climate

U. Port et al.

Table 1. Boundary conditions in the early Eocene climate simulations and in the pre-industrial climate simulations.

	Pre-industrial	Early Eocene
CO ₂ concentration	280 ppm	560 ppm
Methane	0.8 ppm	0.8 ppm
Nitrous oxide	0.288 ppm	0.288 ppm
Orbit	pre-industrial	pre-industrial
Bathymetry and orography	present-day	Bice and Marotzke (2001)
Ice sheets	pre-industrial	none

[Title Page](#)

[Abstract](#)

[Introduction](#)

[Conclusions](#)

[References](#)

[Tables](#)

[Figures](#)

[I◀](#)

[▶I](#)

[◀](#)

[▶](#)

[Back](#)

[Close](#)

[Full Screen / Esc](#)

[Printer-friendly Version](#)

[Interactive Discussion](#)

Radiative forcing by forest and subsequent feedbacks in the early Eocene climate

U. Port et al.

Table 2. Simulations performed with boundary conditions for the early Eocene climate and the pre-industrial climate. The listed vegetation cover is prescribed on all ice-free continents. The values for the land surface albedo refers to snow-free regions. In the desert world, the surface albedo equals the soil albedo. In the forest world, trees cover the soil completely and the albedo of the forest determines land surface albedo.

	Vegetation	Land surface albedo
Dark desert world	none	0.1
Bright desert world	none	0.4
Forest world	100 % tree cover	0.12

[Title Page](#)

[Abstract](#)

[Introduction](#)

[Conclusions](#)

[References](#)

[Tables](#)

[Figures](#)



[Back](#)

[Close](#)

[Full Screen / Esc](#)

[Printer-friendly Version](#)

[Interactive Discussion](#)

Radiative forcing by forest and subsequent feedbacks in the early Eocene climate

U. Port et al.

[Title Page](#)

[Abstract](#)

[Introduction](#)

[Conclusions](#)

[References](#)

[Tables](#)

[Figures](#)

[⏪](#)

[⏩](#)

[◀](#)

[▶](#)

[Back](#)

[Close](#)

[Full Screen / Esc](#)

[Printer-friendly Version](#)

[Interactive Discussion](#)

Table 3. Net radiative forcing by afforesting a bright desert world in the early Eocene climate and the pre-industrial climate. Further, the net feedback parameter and the equilibrium temperature change are listed. The values are derived from the comparison of the respective forest world with the respective bright desert world. The 95 % confidence interval is given. The transient temperature change refers to the temperature difference averaged over the last 30 years of the simulations.

	Early Eocene	Pre-industrial
Radiative forcing [W m^{-2}]	5.8 ± 0.4	5.2 ± 0.5
Feedback parameter [$\text{W m}^{-2} \text{K}^{-1}$]	-1.4 ± 0.1	-0.7 ± 0.1
Equilibrium temperature change [K]	4.1 ± 0.1	7.3 ± 0.7
Transient temperature change [K]	4.2	5.7

Radiative forcing by forest and subsequent feedbacks in the early Eocene climate

U. Port et al.

Table 4. Net radiative forcing by afforesting a dark desert world in the early Eocene climate and in the pre-industrial climate. Further, the net feedback parameter and the equilibrium temperature change are listed. The values are derived from the comparison of the respective forest world with the respective dark desert world. The 95 % confidence interval is given. The transient temperature change refers to the temperature difference averaged over the last 30 years of the simulations.

	Early Eocene	Pre-industrial
Radiative forcing [W m^{-2}]	-3.4 ± 0.4	-3.1 ± 0.5
Feedback parameter [$\text{W m}^{-2} \text{K}^{-1}$]	-0.7 ± 0.1	-0.8 ± 0.2
Equilibrium temperature change [K]	-5.3 ± 0.6	-3.8 ± 0.5
Transient temperature change [K]	-4.2	-3.0

Title Page

Abstract

Introduction

Conclusions

References

Tables

Figures

◀

▶

◀

▶

Back

Close

Full Screen / Esc

Printer-friendly Version

Interactive Discussion

Radiative forcing by forest and subsequent feedbacks in the early Eocene climate

U. Port et al.

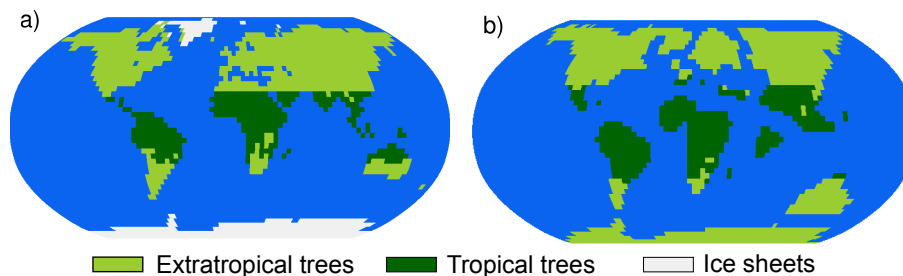


Figure 1. Vegetation cover in the forest world for the pre-industrial climate **(a)** and the early Eocene climate **(b)**. Extra-tropical trees and tropical trees differ concerning their LAI and roughness length.

[Title Page](#)[Abstract](#)[Introduction](#)[Conclusions](#)[References](#)[Tables](#)[Figures](#)[◀](#)[▶](#)[◀](#)[▶](#)[Back](#)[Close](#)[Full Screen / Esc](#)[Printer-friendly Version](#)[Interactive Discussion](#)

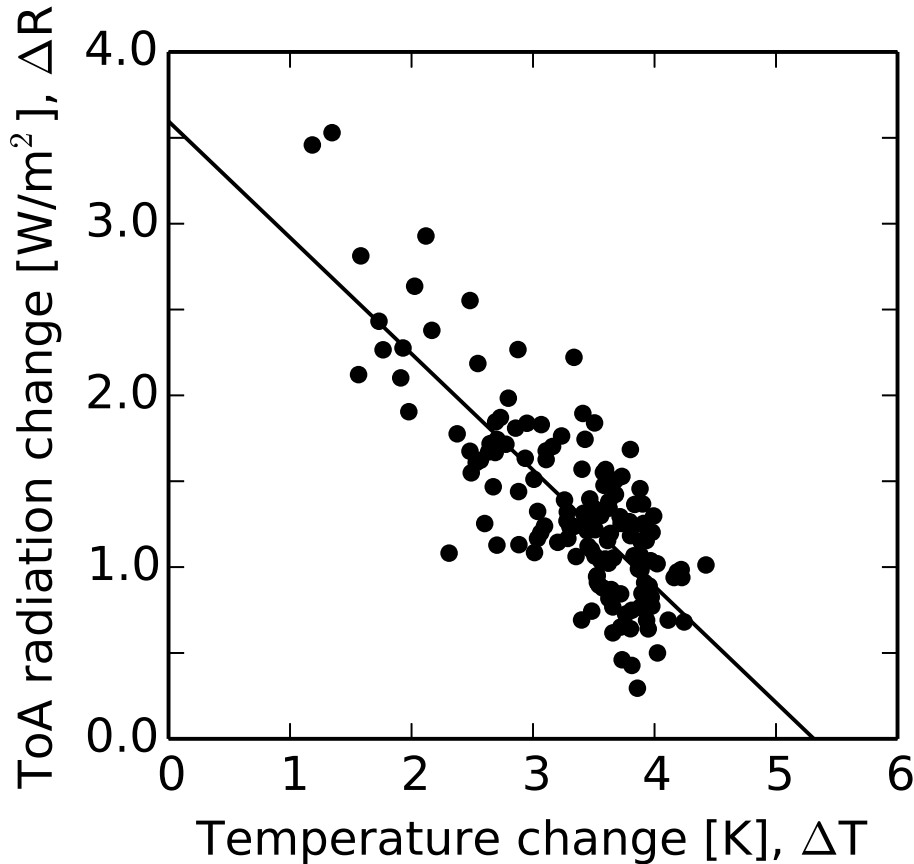


Figure 2. Evolution of radiative flux at the top of the atmosphere with temperature changes at the surface in the dark desert world of the early Eocene climate. At the beginning of the simulation, savanna-like vegetation is replaced by bare soil with an albedo of 0.1. The first 150 simulated years are shown. The black line is the regression line fitted to the first 150 years.

Radiative forcing by forest and subsequent feedbacks in the early Eocene climate

U. Port et al.

Title Page

Abstract

Introduction

Conclusions

References

Tables

Figures



Back

Close

Full Screen / Esc

Printer-friendly Version

Interactive Discussion



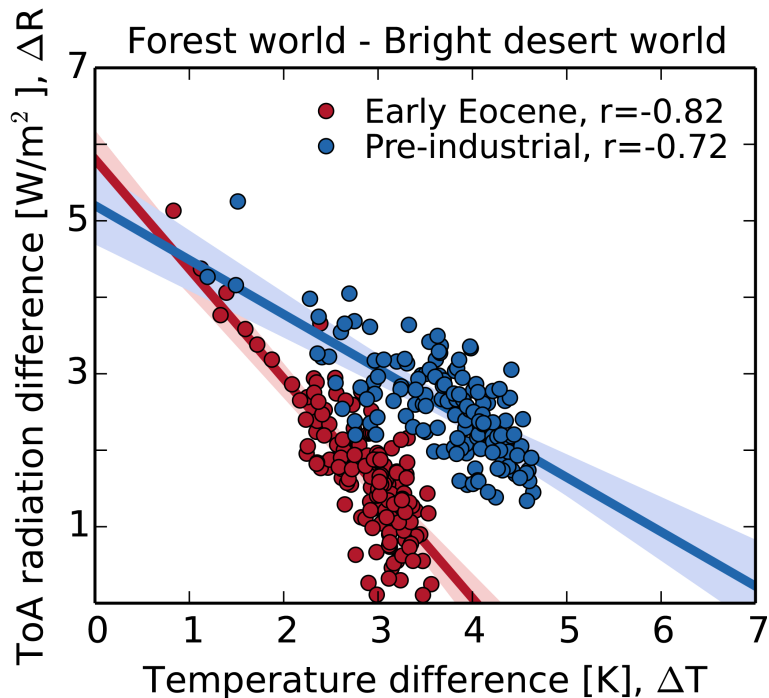


Figure 3. The evolution of differences in the TOA radiative flux between the forest world and the bright desert world with corresponding differences in near-surface temperature. Global annual-mean values are considered. Red and blue points relate to the early Eocene climate and to the pre-industrial climate, respectively. Dark large points and bright small points show the first 150 and the last 250 years, respectively. The regression and the correlation coefficient, r , consider the first 150 years. The shaded areas refer to the 95% confidence interval for the regression lines.

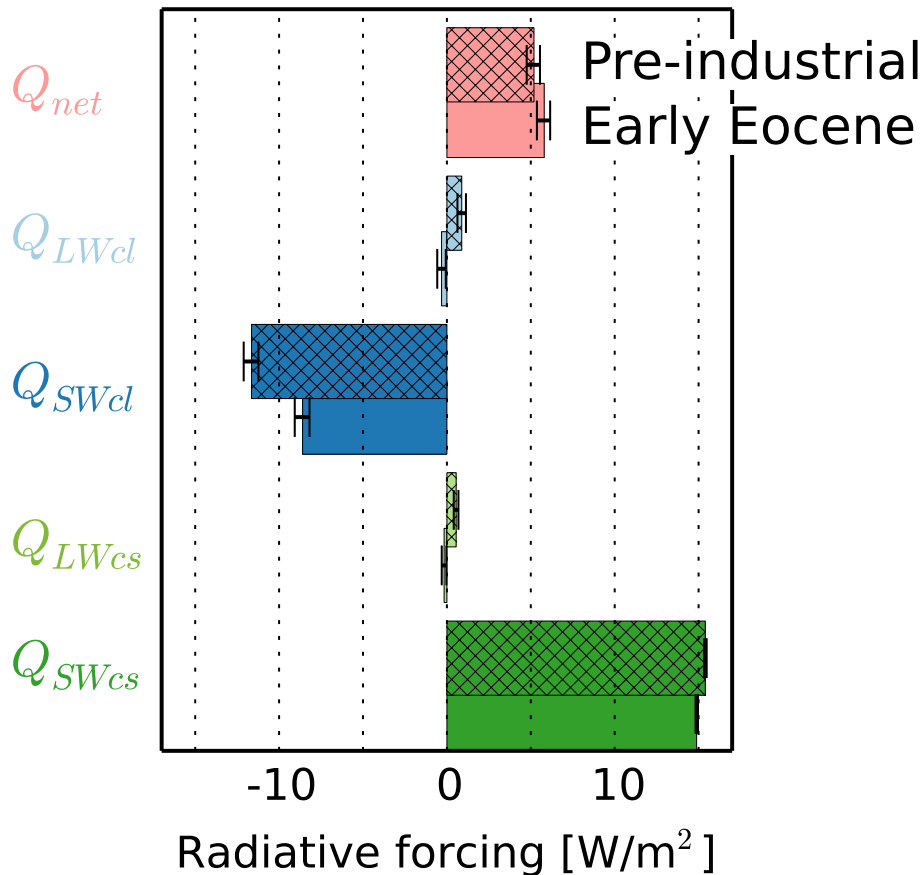


Figure 4. Net radiative forcing and its single components for the comparison of the forest world to the bright desert world. Hatched and plain bars show the radiative forcings for the pre-industrial climate and the early Eocene climate, respectively. The errorbars refer to the 95% confidence interval.

Radiative forcing by forest and subsequent feedbacks in the early Eocene climate

U. Port et al.

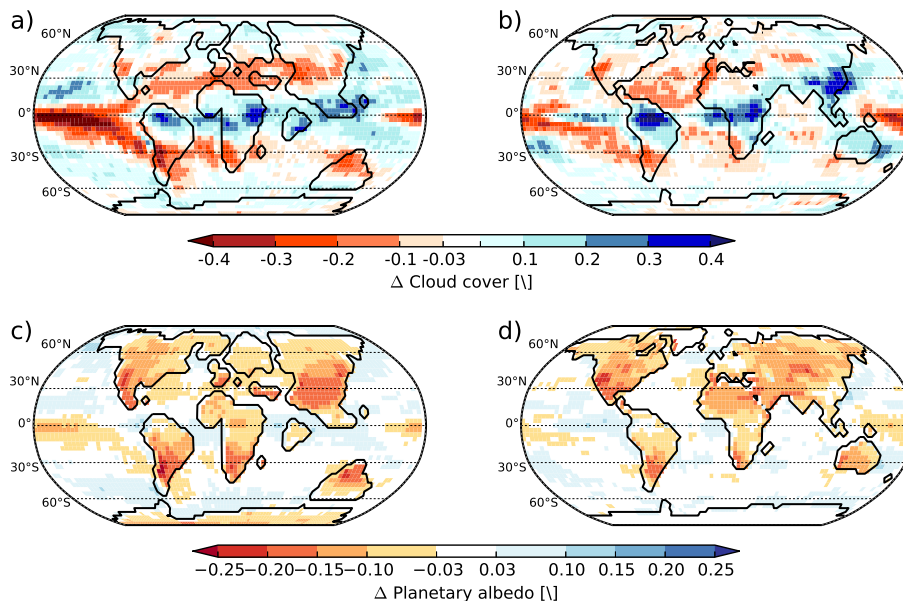


Figure 5. Difference in cloud cover and planetary albedo between the forest and the bright desert world averaged over the first year of the simulations. **(a)** and **(c)** show the differences for the early Eocene climate and **(b)** and **(d)** for the pre-industrial climate.

[Title Page](#)

[Abstract](#)

[Introduction](#)

[Conclusions](#)

[References](#)

[Tables](#)

[Figures](#)

[◀](#)

[▶](#)

[◀](#)

[▶](#)

[Back](#)

[Close](#)

[Full Screen / Esc](#)

[Printer-friendly Version](#)

[Interactive Discussion](#)

Radiative forcing by forest and subsequent feedbacks in the early Eocene climate

U. Port et al.

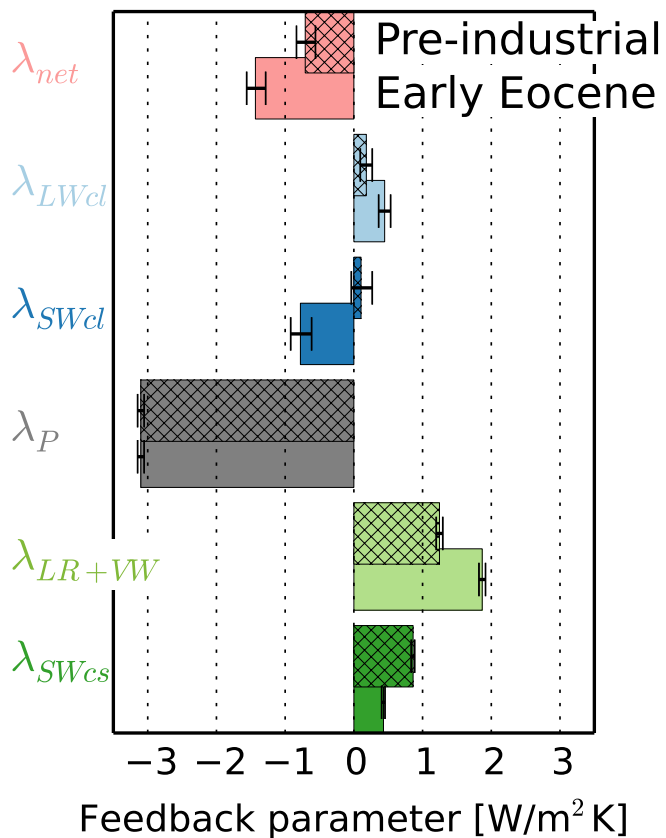


Figure 6. Net feedback parameter and its single components for the comparison of the forest world to the bright desert world. Hatched and plain bars show the feedback parameters for the pre-industrial climate and the early Eocene climate, respectively. The errorbars refer to the 95% confidence interval.

Radiative forcing by forest and subsequent feedbacks in the early Eocene climate

U. Port et al.

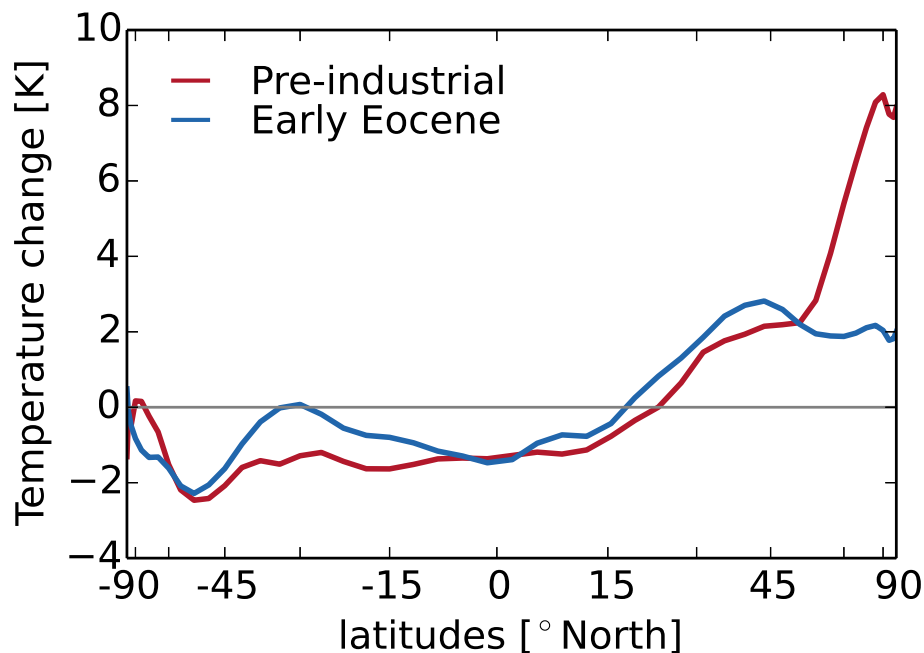


Figure 7. Anomaly of zonal mean temperature change by forest. Global mean temperature difference between the forest world and the desert world are subtracted from differences in zonal mean temperature. Red line and blue line refer to the early Eocene climate and the pre-industrial climate, respectively.

[Title Page](#)[Abstract](#)[Introduction](#)[Conclusions](#)[References](#)[Tables](#)[Figures](#)[◀](#)[▶](#)[◀](#)[▶](#)[Back](#)[Close](#)[Full Screen / Esc](#)[Printer-friendly Version](#)[Interactive Discussion](#)

Radiative forcing by forest and subsequent feedbacks in the early Eocene climate

U. Port et al.

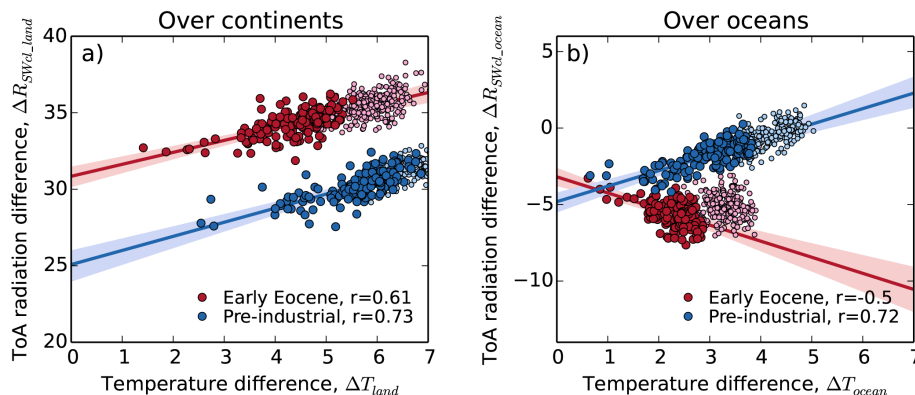


Figure 8. Evolution of the difference in TOA short-wave cloud radiative flux, R_{SWcl} , with differences in near-surface temperature between the forest world and the bright desert world. The evolution of R_{SWcl} is separated in the evolution above the continents (a) and above the oceans (b). Global annual-mean values are considered. Red and blue points relate to the early Eocene climate and to the pre-industrial climate, respectively. Dark large points and bright small points show the first 150 and the last 250 years, respectively. The regression and the correlation coefficient, r , consider the first 150 years. The shaded areas refer to the 95% confidence interval for the regression lines.

Title Page

Abstract

Introduction

Conclusions

References

Tables

Figures

◀

▶

◀

▶

Back

Close

Full Screen / Esc

Printer-friendly Version

Interactive Discussion

Radiative forcing by forest and subsequent feedbacks in the early Eocene climate

U. Port et al.

[Title Page](#)

[Abstract](#)

[Introduction](#)

[Conclusions](#)

[References](#)

[Tables](#)

[Figures](#)

[◀](#)

[▶](#)

[◀](#)

[▶](#)

[Back](#)

[Close](#)

[Full Screen / Esc](#)

[Printer-friendly Version](#)

[Interactive Discussion](#)

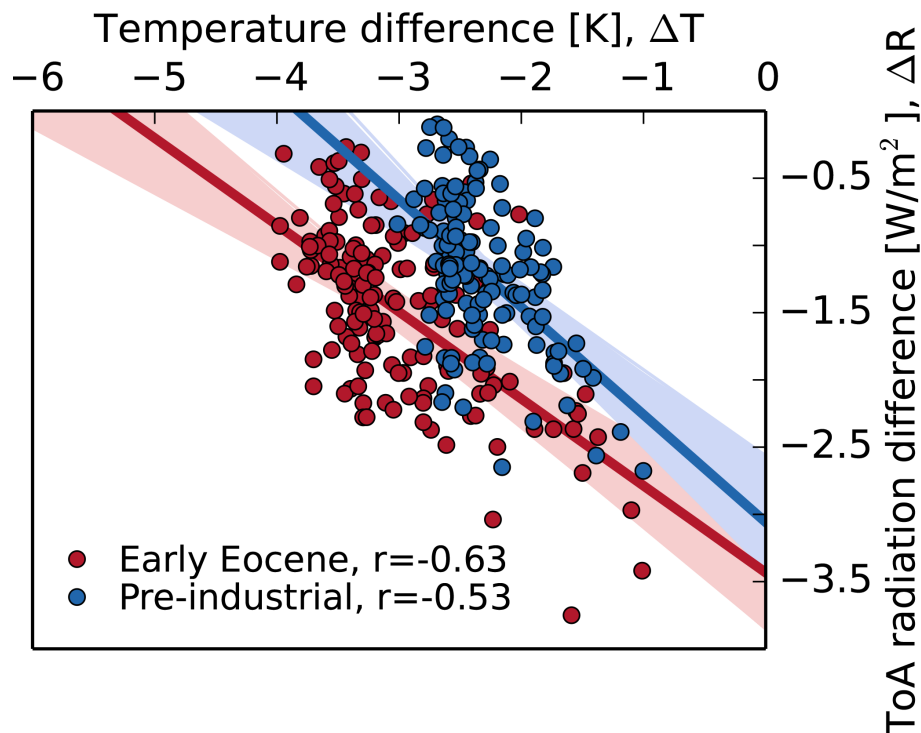


Figure 9. The evolution of differences in the TOA radiative flux between the forest world and the dark desert world with corresponding temperature differences. Global annual mean values are considered. Red and blue points relate to the early Eocene climate and to the pre-industrial climate, respectively. Dark large points and bright small points show the first 150 and the last 250 years, respectively. The regression and the correlation coefficient, r , consider the first 150 years. The shaded areas refer to the 95 % confidence interval for the regression lines.

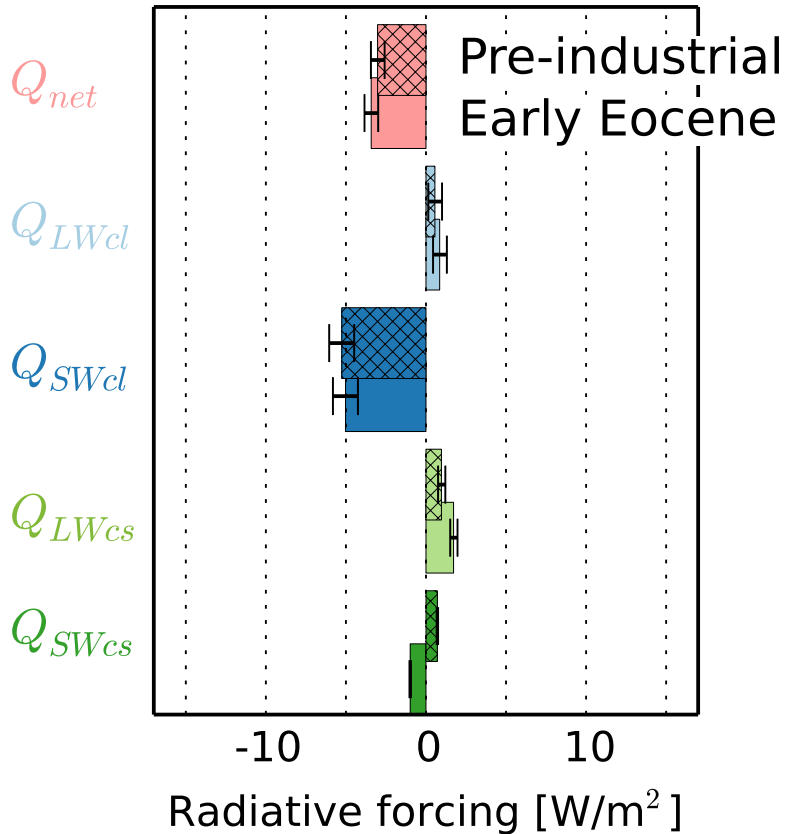


Figure 10. Net radiative forcing and its single components for the comparison of the forest world to the dark desert world. The hatched and the plain bars show the radiative forcings for the pre-industrial climate and the early Eocene climate, respectively. The errorbars refer to the 95 % confidence interval.

[Title Page](#)

[Abstract](#) [Introduction](#)

[Conclusions](#) [References](#)

[Tables](#) [Figures](#)

[◀](#) [▶](#)

[◀](#) [▶](#)

[Back](#) [Close](#)

[Full Screen / Esc](#)

[Printer-friendly Version](#)

[Interactive Discussion](#)



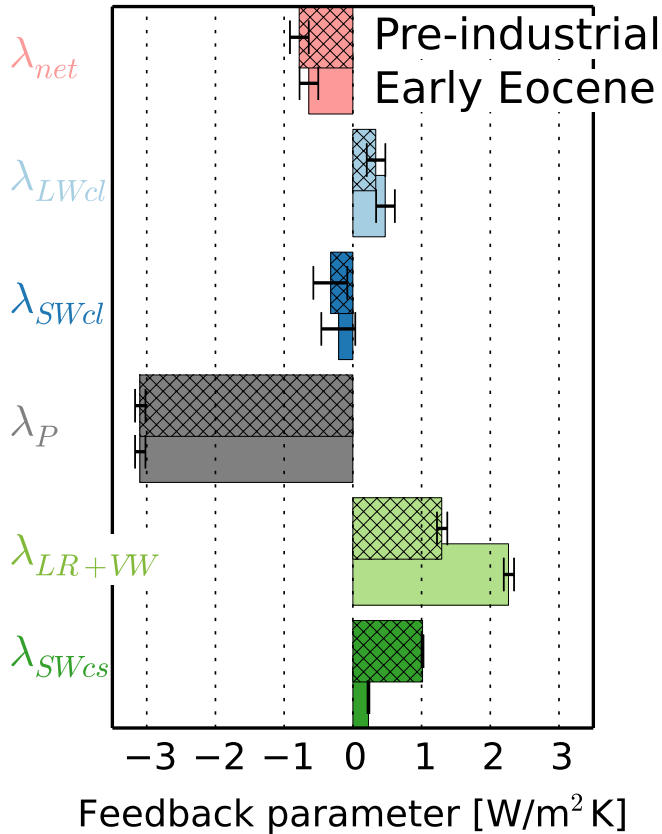


Figure 11. Net feedback parameter and its single components for the comparison of the forest world to the dark desert world. The hatched and the plain bars show the feedback parameters for the pre-industrial climate and the early Eocene climate, respectively. The errorbars refer to the 95 % confidence interval.

Radiative forcing by forest and subsequent feedbacks in the early Eocene climate

U. Port et al.

[Title Page](#)

[Abstract](#)

[Introduction](#)

[Conclusions](#)

[References](#)

[Tables](#)

[Figures](#)

◀

▶

◀

▶

[Back](#)

[Close](#)

[Full Screen / Esc](#)

[Printer-friendly Version](#)

[Interactive Discussion](#)

